



Effect of Bimetallic Doping on the Optoelectronic Properties of Zeolitic Imidazolate Framework-8 (ZIF-8)

Rita A. Daniel-Umeri^{1*}, Mike O. Osiele², Kugbere Emumejaiye¹, Sunday C. Ikpeseni^{3*}

¹Department of Physics, Delta State University of Science and Technology, Ozoro, Delta State, Nigeria

²Department of Physics, Delta State University, Abraka, Delta State, Nigeria

³Department of Mechanical Engineering, Delta State University, Abraka, Delta State, Nigeria

Corresponding authors: ^{3*}scikpeseni@delsu.edu.ng; ^{1*}rdanielumeri@mail.com.

Article Info

Keywords:

ZIF-8, Co/Zn Co-doping,
Optoelectronic Properties,
Photocatalysis

Received 11 January 2025

Revised 20 February 2025

Accepted 24 February 2025

Available online 5 March 2025



<https://doi.org/10.37933/nipes/7.1.2025.3>

eISSN-2682-5821, pISSN-2734-2352

© 2025 NIPES Pub. All rights reserved.

Abstract

Zeolitic Imidazolate Framework-8 (ZIF-8) stands out among other metal-organic frameworks (MOFs) for optoelectronic applications because of its large surface area, high porosity and tunable characteristics. This study examined the impact of bimetallic doping of pristine ZIF-8 with cobalt (Co) and zinc (Zn) in enhancing its performance in devices like photodetectors, solar cells, and light-emitting diodes. UV-VIS spectroscopy, FTIR and SEM were used to analyze the nanocomposites' optical and morphological properties. Optical characterization shows that co-doping enhanced the absorbance thereby reducing the transmittance to an average of 22% making the material appropriate for light-harvesting systems. In addition, bandgap energy decreased from 2.82 eV to 1.25 eV due to impurity band formation improving the optoelectronic response of the material. Furthermore, co-doping increased the refractive index from an average of 1.64 to 2.36, showing higher interactions between light and matter. The dielectric constant was also improved by Co/Zn co-doping suggesting an increase in charge storage as well as polarization crucial for optoelectronic devices. FTIR spectroscopy revealed alterations in the chemical bonds suggesting that the Co and Zn impurities have been successfully incorporated into the ZIF structure. SEM images revealed alterations in the morphology of the composites including increased crystallite size and heterogeneity in appearance due to co-doping and the modification in their composition was confirmed by EDS spectra. Overall, these findings show that bimetallic doping of ZIF-8 nanocomposites with Co and Zn enhanced the optical absorption, charge storage potential and flexibility, making them ideal for sensors, energy harvesting, and photocatalysis.

This article is open access under the CC BY license <http://creativecommons.org/licenses/by/4>.

1.0 Introduction

Metal-organic frameworks (MOFs) are a type of crystalline and porous materials that are appealing due to their exceptional composition and structural flexibility, high specific surface areas ($1000\text{--}10,000\text{ m}^2\text{ g}^{-1}$), tunable pore size and defined morphology making of them suitable for a wide range of applications. They are composed of organic ligands and metal ions/clusters under the action of a coordination bond. Zeolitic imidazolate framework-8 (ZIF-8) is one type of MOF that stands out due to the sodalite (SOD) topology that it possess which creates a structure that is highly porous having large a surface area and pore size of approximately 11.6 \AA . This tunable pore enables adsorption and transport of ions easily. [1, 2] [3,4].

In ZIF-8, zinc ions are tetrahedrally coordinated with nitrogen atoms from 2-methylimidazole ligands [3, 5] this establishes a three-dimensional framework that is stable due to strong metal-ligand bonds. The open framework and high pore volume facilitate guest molecule diffusion and high loading capacity for various applications [6,7] such as gas storage and separation [8], catalysis [7], drug delivery [9], sensors [10] and environmental remediation [11].

In recent times, the interest in the fabrication of ZIF-8 for use in optoelectronic devices has been on the increase because of its ability to create charge carriers under light. However, its large bandgap limits visible light response. Meanwhile, metal doping techniques are being explored to address this issue [12-14]. One of the strategies that have been adopted to address the limitation of ZIF-8 and enhance its optoelectronic performance is co-doping strategies, especially with transition metals such as cobalt (Co) and zinc (Zn). These metals introduce new electronic states in the ZIF structure that improve its light response in the visible spectrum. Pristine ZIF-8 has a relatively wide bandgap, which limits its ability to absorb light in the visible spectrum. Incorporating cobalt and zinc in the framework introduces impurity states that reduce the bandgap, significantly improving light absorption and modifies the structural and morphological properties which usually results in larger and more heterogeneous particle sizes. In addition, Co/Zn doping enhances the dielectric properties of ZIF-8. These improvements boost the material's optoelectronic properties [15-19].

Bimetallic metal-organic frameworks (BMOFs) are hybrid materials that combine two MOFs' characteristics to produce nanomaterials with special chemical and structural qualities. . The architecture of bimetallic MOFs can be classified into two main categories according to the metal distribution namely solid solution and core-shell structures. Compared to their monometallic counterparts, bimetallic MOFs exhibit improved capabilities and a synergistic impact making them suitable in many applications such as gas adsorption, catalysis, energy storage and conversion, and luminescence sensing. The choice of the metal combinations and ratios allows for the tuning of bimetallic ZIFs' pore size, absorption control characteristics, acidity/basicity, and surface area and redox characteristics [20, 21]. The tailoring of MOF electronic properties could be performed as a function of metal node engineering allowing for fine-tuning of conductivity, band gap, and other electrical characteristics depending on the desired application [22]. MOFs may have superior electrical conductivity for a range of applications, including resistive sensors, supercapacitors, semiconductors, and thermoelectrics, if various metals are mixed in their secondary-building units (SBUs) [20, 23].

Li et al. [24] developed ZnO@C-N-Co core-shell nanocomposites derived from Zn/Co ZIF for the degradation of methyl orange (MO). Upon calcination of the Zn/Co ZIF at 600 °C, ZnO nanoparticles formed from the ZIF-8 shell aggregated and moved to the hollow cavity, while the internal Co nanoparticles migrated to the N-C shell. This process resulted in the creation of a unique ZnO@C-N-Co core-shell structure. Nguyen et al. [25] synthesized Co/Zn-ZIF-8 at room temperature and observed a lower HOMO-LUMO gap when compared with pristine ZIF-8 due to charge transfer from organic ligands to cobalt centers. The nanocomposites also demonstrated high hydrolytic stability and photocatalytic efficiency in degrading indigo carmine (IC) dye under solar-simulated irradiation. Xu et al. [26] fabricated co-doped ZIF-8 (Co_xZn_{1-x}-ZIF-8) with varying Co²⁺ and Zn²⁺ ratios to enhance its photocatalytic performance. The results show that the nanoamaterial absorbed in the visible light, improving methylene blue degradation.

Butova et al. [27] tested iodine sorption properties in ZIF-8 samples with varying Zn/Co ratios using excess sublimated iodine. They observed that co-doping resulted in a reduced thermal stability of the samples after iodine saturation. The Fe-and-N co-doped Fe-ZIF-8 metal-organic framework was synthesized by Luo et al. [28], they used a photocatalyst to decompose organic dyes under visible light irradiation. The results show that its band gap drops sharply from 5.11 eV to 2.17 eV and possesses stronger absorption in visible light region

Wang, et al. [29] prepared Co/Fe co-doped ZIF-8 for Cu²⁺ ions capacitive deionization The density functional theory calculations demonstrated that the co-doping of Co and Fe remarkably increase the adsorption energies of Cu²⁺ ions, leading to excellent selectivity, which indicates that CoFe-NC composites can be a desired CDI electrode material. Mehrehjedy et al. [30] studied the optical properties of Fe₃O₄, ZIF-8, ZIF-67, and Co20%-ZIF-8 using diffuse reflectance spectroscopy (DRS.) The results revealed that cobalt doping in ZIF-8 (Co-ZIF-8) successfully reduced its band gap from 5.15 eV to 1.98 eV, indicating an enhancement in photocatalytic activity under visible light.

Several methods have been used to synthesize ZIF-8 metal-organic frameworks such as hydrothermal [31], sonochemical method [32], microwave-assisted [33], Co-precipitation method [34, 35] etc. A facile wet chemical method of synthesis used for this work is the direct combination method (DCM). It is a straightforward and scalable technique for synthesizing metal-organic frameworks (MOFs). In this approach, metal salts and organic linkers are directly mixed in a solvent under controlled conditions, such as pH, concentration, and reaction time, typically at room temperature. The metal salts and organic linkers react through coordinate bonds during self-assembly to create the required MOF structure. DCM is a useful and accessible technique for researchers including beginners [36, 37].

The objective of this study is to examine how cobalt (Co) and zinc (Zn) bimetallic doping influence the optoelectronic characteristics of Zeolitic Imidazolate Framework-8 (ZIF-8) to enhance its usefulness for technological applications. Optical properties such as absorbance, transmittance, reflectance, bandgap energy, refractive index and the real and imaginary part of the dielectric constant will be considered. In addition, the changes in the crystal structure and surface morphology were analyzed. These modifications due to co-doping aim to enhance ZIF-8's performance in solar cells, LEDs, photodetectors, sensors, and photocatalysis.

2. Materials and Method

A. Materials

The materials use for the fabrication include zinc nitrate hexahydrate ($\text{Zn}(\text{NO}_3)_2 \cdot 6\text{H}_2\text{O}$), cobalt nitrate hexahydrate ($\text{Co}(\text{NO}_3)_2 \cdot 6\text{H}_2\text{O}$), Trimethylamine ($\text{C}_3\text{H}_9\text{N}$) and 2-Methylimidazole ($\text{C}_4\text{H}_6\text{N}_2$). Distilled water, methanol and Dimethyl sulfoxide, DMSO ($\text{C}_2\text{H}_6\text{OS}$) were used as the solvents.

B. Method

To synthesize ZIF-8, 1.0 g of $\text{Zn}(\text{NO}_3)_2 \cdot 6\text{H}_2\text{O}$ was dissolved in 50 ml of distilled water and stirred for 30 minutes (Solution A). Separately, 2.7 g of 2-Methylimidazole (2-MeIM) was dissolved in 50 ml of distilled water, stirred for 15 minutes, and mixed with 4 ml of Trimethylamine (TMA) to promote ligand deprotonation (Solution B). The two solutions were combined and stirred for 45 minutes using a magnetic stirrer, forming a cream-colored mixture. ZIF-8 crystals were collected by centrifuging the mixture at 6500 rpm for one hour, followed by washing and a second centrifugation for 30 minutes. The cleaned crystals were dried at 200°C for three hours and stored in an airtight container.

For the fabrication of Co/Zn/ZIF-8, 0.5 g of ZIF-8 powder was dissolved in 10 ml of dimethylsulfoxide (DMSO) and stirred for one hour. 0.6 g each of $\text{Co}(\text{NO}_3)_2 \cdot 6\text{H}_2\text{O}$ and $\text{Zn}(\text{NO}_3)_2 \cdot 6\text{H}_2\text{O}$ were also dissolved separately in 10 ml of dimethylsulfoxide (DMSO). The three solutions were mixed and stirred for two hours to form the MOF, followed by centrifugation, washing, and drying in a furnace at 200°C . The resultant nanocomposites was stored in an air-tight container to prevent contamination.

C. Material Characterization

The optical properties were assessed using a UV-VIS-NIR (UV-1800 series), while the chemical bonds and functional groups in the materials were determined using a JASCO-FTIR (FT/IR-6600) spectrometer. Surface morphology was analyzed by scanning electron microscopy (SEM) coupled with energy-dispersive spectroscopy (EDS) (MRA3 TESCAN).

3.0. Results and Discussion

A. Optical analysis

The results obtained from the optical characterization of the fabricated nanocomposites using UV-VIS-NIR (UV-1800 series) spectroscopy in the wavelength range between 300 and 800 nm were used to plot the following graphs.

The absorbance graph for pristine and Co/Zn co-doped ZIF-8 as shown in Fig 1(a) reveal peaks at 320 nm and 340 nm which is linked to electronic transitions involving zinc and imidazolate. The spectral also showed changes in the peak intensity and an increase in the absorbance because of the introduction of dopants in the ZIF-8 thereby enhancing its potential for sensing and photocatalysis [38, 39].

The increase in absorbance in the Co/Zn co-doped ZIF-8 is made possible because of the synergistic impact of Co^{2+} and Zn^{2+} ions. Since ZIF-8 is already composed of zinc ions (Zn^{2+}), doping with additional zinc may not have a dramatic change but can change the local coordination environment around the metal centers which may affect the interaction between the metal and the organic linkers influencing the overall light absorption properties of the material. The presence of cobalt ions (Co^{2+}) on the other hand introduces electronic states that provide new pathways for electron excitation and facilitating light absorption at wavelengths that ZIF-8 alone could not efficiently absorb. The optical characteristics may be impacted by the ability of Co^{2+} ions' to interact with the surrounding ZIF-8 framework which changes the charge distribution. This alteration can lead to new absorption peaks or shifts in existing ones, thereby increasing the nanocomposites capacity to absorb light, particularly in the visible range. This helps in improving photon harvesting which are relevant to the performance of photovoltaic and photocatalytic devices [15, 20, 29, 30].

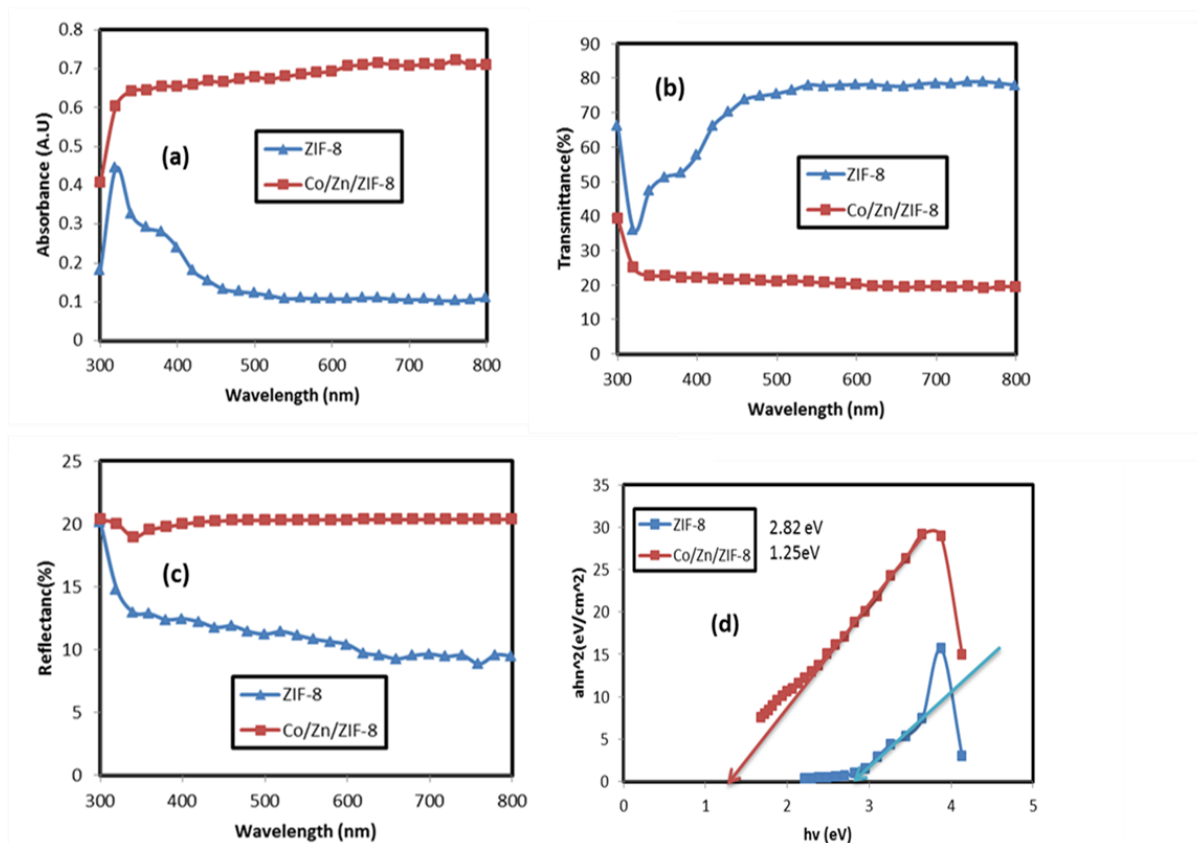


Fig. 1. (a) Absorbance spectrum of pristine ZIF-8 and Co/Zn/ZIF-8 (b) Transmittance spectrum of pristine ZIF-8 and Co/Zn/ZIF-8 (c) Reflectance spectrum of pristine ZIF-8 and Co/Zn/ZIF-8 (d) Bandgap of pristine ZIF-8 and Co/Zn/ZIF-8

In photovoltaic devices, enhanced absorbance in the UV-Visible region can improve photon harvesting and power conversion efficiency as observed in materials like perovskite solar cells (PSCs) and organic solar cells (OSCs). Similarly, the enhanced absorption in the visible-NIR region can increase photon absorption efficiency improving solar-driven catalytic activity [40, 41].

The graph of transmittance against wavelength for pristine ZIF-8 and Co and Zn co-doped ZIF-8 is shown in fig 1(b). Since the transmittance spectrum provides information complementary to the absorbance spectrum it means that high absorbance peaks translate to low transmittance valleys, and vice versa. An average transmittance value of 71% was recorded by pristine ZIF-8 making it ideal for photovoltaics, LEDs, and sensors while co-doping reduced the transmittance below 22% across the visible region due to the introduction of new electronic states by the incorporation of cobalt ions (Co^{2+}) into the ZIF-8 framework, creating structural defects or localized electronic states within the material. These defects or states can scatter light, causing a reduction in transmittance, hence enhancing its suitability in applications, such as, photocatalysis, optical fibers and luminescent devices. [38, 39].

Figure 1(c) displays the graph of reflectance against wavelength for both pure ZIF-8 and Co/Zn ZIF-8. Reflectance quantifies the quantity of light reflected from a material's surface.

From the graph, pristine ZIF-8 has an average reflectance of 11% which increases to 20% with the addition of both Co and Zn. Both materials exhibit low reflectance, suitable for optoelectronic applications like solar cells and photodetectors by minimizing internal reflection losses [43, 44].

The graph of $(ah\nu)^2$ Vs $h\nu$, which represents the bandgap for both pristine ZIF-8 and Co and Zn co-doped ZIF-8, is shown in Fig. 1(d). The band gap (E_g) determines the optical and electronic performance of most materials.

The value of the optical band gap can be obtained from the fundamental absorption of the material which corresponds to the excitation of electrons from the valence band to the conduction band. The band gap was determined from the intersect of straight line portion of $(\alpha h\nu)^2$ versus $h\nu$.

From the Tauc's plot the bandgap reduced from 2.82 eV for pristine ZIF-8 to 1.25 eV for Co/Zn co-doped ZIF-8. The reduction of the bandgap from 2.82 eV to 1.25 eV upon Co/Zn doping suggest that new impurity states have been introduced in the electronic structure of ZIF-8. When Co^{2+} is substituted into the ZIF-8 lattice, there is a strong hybridization between Co d-orbitals and the ligand π -system leading to the formation of mid-gap states within the bandgap which reduces the energy required for electronic transitions. Zn^{2+} on the other hand maintains the wide bandgap but causes changes in the local electronic states. In addition, because Co^{2+} distorts the crystal lattice slightly, the Co-N bond length is increased which alters the phonon interactions, thereby affecting its optoelectronic properties while Zn stabilizes the lattice and minimizes defect formation. Co^{2+} and Zn^{2+} bimetallic substitution modifies the pore size and metal-ligand interactions, enhancing guest adsorption and catalytic activity particularly in optoelectronic and photoelectrochemical applications [26, 44, 45, 46].

A study conducted by Vatani et al. [21] shows that the bandgap energy of bimetallic of Zn/ Co ZIF-8 particles was almost close to that of mono Co-ZIF-8. This means the cobalt ions mainly control the optical properties of the bimetallic Zn/ Co ZIF particles. The obtained bandgap values are 3.46 and 3.4 eV for Zn / Co ZIF-8 and Co-ZIF-8 respectively. Li et al., [24], developed a lanthanide-doped nanoparticles (LDNPs) coated with Fe/Mn bimetal-doped ZIF-8 (LDNPs@Fe/Mn-ZIF-8) the dual doping of $\text{Fe}^{2+}/\text{Mn}^{2+}$ markedly decrease the bandgap of the ZIF-8 photosensitizer from 5.1 to 1.7 eV.

The value obtained in this study can be compared to the bandgap value of 1.241eV obtained by Baghban et al. [47] using DFT calculation.

Fig. 2(a) illustrates the refractive index (n) versus photon energy for pristine ZIF-8 and Co/Zn-doped ZIF-8. The refractive index indicates the material's interaction with light including absorption, transmission, and reflection and this is closely tied to its optoelectronic performance. It represents the frequency range where the films are weakly absorbing. The plot shows that co-doping the ZIF-8 MOF increased the refractive index from an average value of 1.64 to 2.36 indicating a stronger interaction with light. The refractive index (n) of a material has a close relationship to its electronic polarizability, which describes how easily electrons in the material can be displaced by an external electric field such as light [48]. When cobalt (Co^{2+}) is incorporated into the ZIF-8 framework alongside zinc (Zn^{2+}), it alters the local electronic environment as a result of changes in the bandgap energy and the extinction coefficient, therefore increasing the nanocomposite's ability to polarize in response to light and consequently, a higher refractive index [49]. The high refractive index values in the visible range indicate that they are particularly useful for optoelectronic applications, such as photovoltaics, solar cells, and sensors, where strong light confinement and manipulation are needed [16, 50, 51].

In devices like thin film solar cells, which requires light trapping techniques to increase the light absorption and modify the optical response, materials with a high refractive index can help trap light more effectively [52,53].

The graph of the extinction coefficients for Co/Zn/ZIF-8 and pristine ZIF-8 is shown in Fig. 2(b). The extinction coefficient (k) of a MOF is the amount of light it can absorb per unit distance. This affects the stability, charge generation as well as the design of the device. From the plot, the k value of both nanocomposites is less than 0.1 indicating that they absorb light minimally which translates to high transparency appropriate for applications like protective coatings and light-transmitting windows [54, 55].

The dielectric properties of pristine ZIF-8 and Co/Zn-doped ZIF-8 are shown in Fig. 2(c) and Fig. 2(d). From the graph, the real part of the dielectric constant (ϵ_r) which is associated with energy storage and polarization was found to increase from 2.62 to 5.34 upon co-doping suggesting that responsiveness to visible and infrared light has been enhanced and the bandgap reduced making it useful for devices like photodetectors and photovoltaics. Similarly, the imaginary part (ϵ_i) which is associated with light absorption and energy loss increased from 0.183 to 0.220 with Co and Zn co-doping. These properties make it suitable for applications such as light-harvesting and photothermal materials [56, 57].

When Co^{2+} and Zn^{2+} are incorporated into the ZIF-8 framework it results in a metal-ligand interaction that increases the nanocomposites polarizability. Co^{2+} with partially filled d-orbitals can create a higher degree of electronic polarization under an applied electric field improving its ability to store charge thereby enhancing the dielectric constant. In photovoltaic and photodetector devices, a high dielectric constant can enhance charge carrier separation and minimize recombination losses, leading to improved device performance [58, 59, 60].

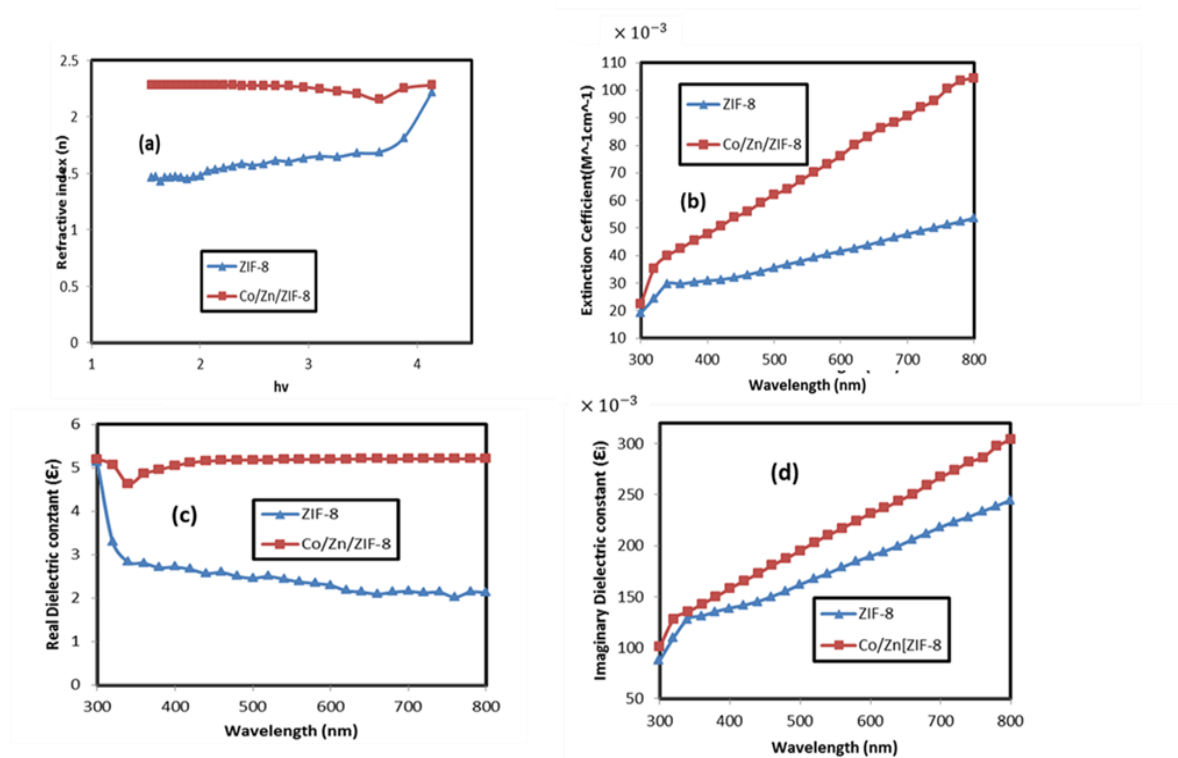


Fig. 2. (a)Refractive index of pristine ZIF-8 and Co/Zn/ZIF-8 (b) Extinction coefficient of pristine ZIF-8 and Co/Zn/ZIF-8 (c)Real dielectric constant of pristine ZIF-8 and Co/Zn/ZIF-8 (d)Imaginary dielectric constant of pristine ZIF-8 and Co/Zn/ZIF-8

B. FTIR results

FTIR analysis on the nanocomposites was conducted over a wavenumber range of 4500–500 cm⁻¹ using a JASCO FT/IR-6600 spectrometer to study the molecular structure, functional groups, and the type of bond between the chemical compositions.

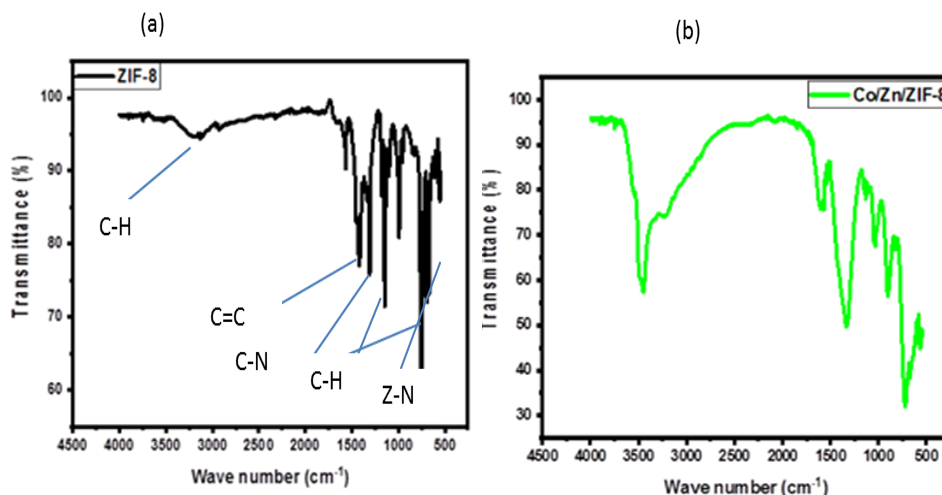


Fig. 3. (a)FTIR of ZIF-8 (b) FTIR of Co/Zn/ZIF-8

Fig. 3 displays the FTIR spectra of pristine ZIF-8 and Co/Zn/ZIF-8. As shown in 3(a), pristine ZIF-8 has distinct bands at 3135, 1650, 1150, 995, 760, 690, and 500 cm⁻¹. The aromatic and aliphatic C-H asymmetrical stretching vibrations were linked to the peak at 3135 cm⁻¹. The 1650 cm⁻¹ band was attributed to the stretching vibration of C=C. The band near 1150 cm⁻¹

represented the C-N stretching mode of the aromatic compound. While the peaks around the wavenumbers of 995 cm^{-1} , 760 cm^{-1} , and 690 cm^{-1} can be assigned to the out-of-plane bending vibration of the imidazole ring, vibration due to C-H bending modes and out-of-plane bending vibrations of the aromatic rings present in the 2-methylimidazole ligand. Another peak was observed at 500 cm^{-1} , a low-frequency band, and this suggests Zn-N metal-ligand vibrations, which confirms the zinc ion coordination and the nitrogen atoms of the imidazole rings. The slight shifts and changes in peak intensity and width as observed in Fig. 3(b) shows that Co and Zn have been successfully integrated into the ZIF-8 framework. The structural bonds observed in the nanocomposites support their potential for optoelectronic applications [2122,56].

C. SEM/EDS Analysis

SEM-EDS analysis has been conducted on the fabricated nanocomposites to examine their morphology and elemental distribution using MIRA3 TESCAN. The resulting MOFs exhibited a uniform surface structure, free from pinholes and cracks. Our observations indicate that the incorporation of the doping metal significantly influences the acquired morphology.

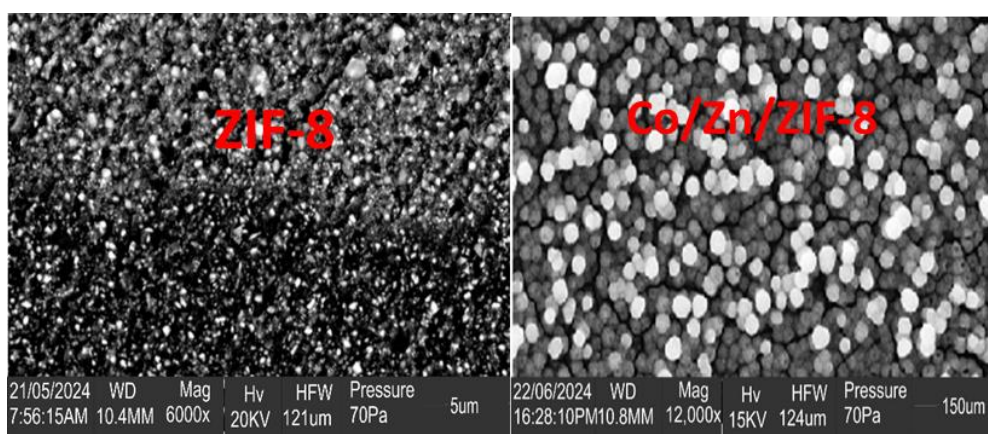


Fig. 4. SEM micrograph of ZIF-8 and Co/Zn/ZIF-8

Figure 4 shows the SEM images of pristine ZIF-8 and Co/Zn/ZIF-8 which displayed the changes in the morphology of ZIF-8 as a result of cobalt and zinc co-doping. Pristine ZIF-8 consists of crystalline nanograins that are evenly distributed and closely packed. Co/Zn/ZIF-8 showed larger particles with mixed colorations indicating that changes have occurred in the chemical composition and structure of the nanocomposites. The observed features which may likely be caused by variations in growth rates or selective cobalt ion adsorption, suggest enhanced conductivity and light absorption beneficial for optical and electronic properties. This makes Co/Zn/ZIF-8 a promising material for energy harvesting, photocatalysis, and sensor applications [56, 60].

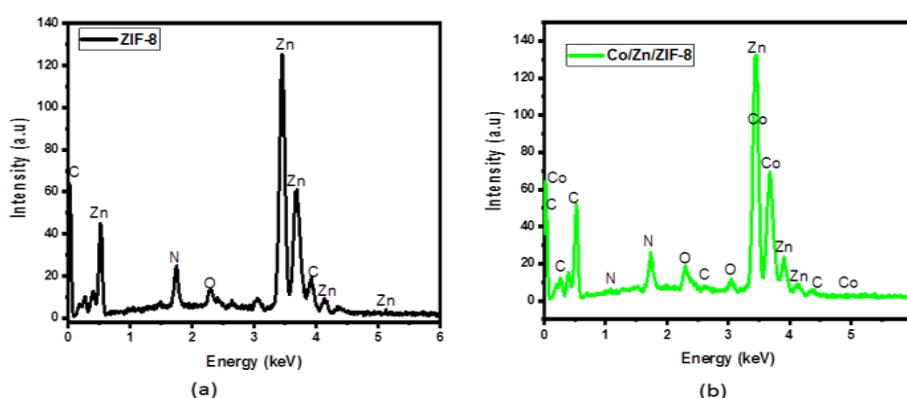


Fig. 5. EDS spectrum. (a) ZIF-8 (b) Co/Zn/ZIF-8

Fig. 5 shows the EDS spectra for ZIF-8 and Co/Zn/ZIF-8 nanocomposites. In pristine ZIF-8 (a), peaks for zinc, nitrogen, oxygen, and carbon confirm the expected elemental composition which is essential for consistent optoelectronic performance. The zinc (Zn) provides structural stability through its four-fold arrangement with imidazole ligands. The oxygen peak suggests residual hydroxyl groups from synthesis. In the Co/Zn/ZIF-8 spectrum, fewer zinc peaks reflect cobalt's substitution, with clear

cobalt peaks indicating successful doping. Increased nitrogen peaks arise from imidazolate linkers bonding with both Zn and Co. Additional oxygen peaks may relate to residual solvents or framework defects. Cobalt doping reduces the bandgap, enhancing light absorption and conductivity, which benefits photocatalytic and sensing applications [15, 12, 13].

4.0. Conclusion

In this work, pristine ZIF-8 and Co/Zn co-doped ZIF-8 have been studied to determine how co-doping can affect the optical, structural, and morphological characteristics for optoelectronic applications. From optical studies, co-doping reduced the bandgap from 2.82 eV to 1.25 eV, improving its light absorption and optoelectronic performance. An increase in the refractive index and extinction coefficient indicated stronger light-matter interactions. FTIR spectrum confirmed the integration of Co and Zn into the ZIF-8 framework while preserving important functional groups. SEM revealed larger particles with mixed coloration in the co-doped material which reflects improved light absorption and conductivity. The elemental compositions of the nanocomposites were verified using EDS analysis. The results show that Co/Zn co-doped ZIF-8 can be utilized as a viable material for energy-harvesting technology, sensors, and photocatalysis. However, there arise the issues of long-term stability and scalability under some operating conditions. Exposure of the nanomaterial to UV radiation may lead to photo-degradation and potential performance losses during prolonged thermal cycling. This can be addressed by embedding the ZIF-8 framework in a protective matrix like graphene to prevent the nanomaterial's degradation and preserve its photoactive properties over extended periods. In addition, employing advanced methods like time-resolved photoluminescence and transient absorption spectroscopy that can offer detailed insights into the charge carrier dynamics, excited-state behaviors and the composites stability are necessary. These methods could clarify whether the impurities acted as recombination centres or facilitated efficient charge separation which can enhance the bimetallic ZIF-8 suitability for optoelectronic and photocatalytic applications. Moreover, large-scale synthesis could present challenges such as dopant uniformity, reaction time control and solvent usage, but employing methods such as continuous flow synthesis, hydrothermal, or solvothermal techniques offer scalable solutions

References

- [1] Jia, T., Gu, Y., & Li, F. (2022). Progress and potential of metal-organic frameworks (MOFs) for gas storage and separation: A review. *Journal of Environmental Chemical Engineering*, 10(5), 108300. <https://doi.org/10.1016/j.jece.2022.108300>
- [2] Yang, L., Karimi, M., Gong, Y., Dai, N., Safarifarid, V., & Jiang, H. (2021). Integration of metal-organic frameworks and covalent organic frameworks: Design, synthesis, and applications. *Matter*, 4(7), 2230–2265. <https://doi.org/10.1016/j.matt.2021.03.022>
- [3] Dai, H., Yuan, X., Jiang, L., Wang, H., Zhang, J., Zhang, J., & Xiong, T. (2021). Recent advances on ZIF-8 composites for adsorption and photocatalytic wastewater pollutant removal: Fabrication, applications and perspective. *Coordination Chemistry Reviews*, 441, 213985. <https://doi.org/10.1016/j.ccr.2021.213985>
- [4] Wang, S., Luo, L., Wu, A., Wang, D., Wang, L., Su, Z., & Tian, C. (2024). Recent advances in tailoring zeolitic imidazolate frameworks (ZIFs) and their derived materials based on hard template strategy for multifunctional applications. *Coordination Chemistry Reviews*, 498, 215464. <https://doi.org/10.1016/j.ccr.2023.215464>
- [5] Zhou, K., Mousavi, B., Luo, Z., Phatanasri, S., Chaemchuen, S., & Verpoort, F. (2017). Characterization and properties of Zn/Co zeolitic imidazolate frameworks vs. ZIF-8 and ZIF-67. *Journal of Materials Chemistry A*, 5(3), 952–957. <https://doi.org/10.1039/c6ta07860e>
- [6] Annamalai, J., Murugan, P., Ganapathy, D., Nallaswamy, D., Atchudan, R., Arya, S., Khosla, A., Seetharaman, B., & Sundramoorthy, A. K. (2022). Synthesis of various dimensional metal organic frameworks (MOFs) and their hybrid composites for emerging applications – A review. *Chemosphere*, 298, 134184 <https://doi.org/10.1016/j.chemosphere.2022.134184>
- [7] Qin, Y., Han, X., Li, Y., Han, A., Liu, W., Xu, H., & Liu, J. (2020). Hollow mesoporous metal-organic frameworks with enhanced diffusion for highly efficient catalysis. *ACS Catalysis*, 10(11), 5973–5978. <https://doi.org/10.1021/acscatal.0c01432>
- [8] Mu, L., Liu, B., Liu, H., Yang, Y., Sun, C., & Chen, G. (2012). A novel method to improve the gas storage capacity of ZIF-8. *Journal of Materials Chemistry*, 22(24), 12246. <https://doi.org/10.1039/c2jm31541f>
- [9] Wang, Q., Sun, Y., Li, S., Zhang, P., & Yao, Q. (2020). Synthesis and modification of ZIF-8 and its application in drug delivery and tumor therapy. *RSC Advances*, 10(62), 37600–37620. <https://doi.org/10.1039/d0ra07950b>
- [10] Paul, A., Banga, I., Muthukumar, S., & Prasad, S. (2022). Engineering the ZIF-8 pore for electrochemical sensor applications—A Mini Review. *ACS Omega*, 7(31), 26993–27003. <https://doi.org/10.1021/acsomega.2c007370>
- [11] Mo, Z., Tai, D., Zhang, H., & Shahab, A. (2022). A comprehensive review on the adsorption of heavy metals by zeolite imidazole framework (ZIF-8) based nanocomposite in water. *Chemical Engineering Journal*, 443, 136320 <https://doi.org/10.1016/j.cej.2022.136320>
- [12] Liang, Y., Cheng, L., Zhang, S., Yang, S., Liu, W., Xie, J., Li, M., Chai, Z., Wang, Y., & Wang, S. (2022). Boosting the optoelectronic performance by regulating exciton behaviors in a porous semiconductive metal-organic framework. *Journal of the American chemical society*, 144(5), 2189–2196. <https://doi.org/10.1021/jacs.1c11150>
- [13] Zheng, Y., Sun, F., Han, X., Xu, J., & Bu, X. (2020). Recent progress in 2D metal-organic frameworks for optical applications. *Advanced optical materials*, 8(13). <https://doi.org/10.1002/adom.202000110>
- [14] Abdollahi, B., Najafidoust, A., Asl, E. A., & Sillanpää, M. (2021). Fabrication of ZIF-8 metal organic framework (MOFs)-based CuO-ZnO photocatalyst with enhanced solar-light-driven property for degradation of organic dyes. *Arabian Journal of Chemistry*, 14(12), 103444 <https://doi.org/10.1016/j.arabj.2021.103444>
- [15] Taheri, M., Enge, T. G., & Tsuzuki, T. (2020). Water stability of cobalt doped ZIF-8: a quantitative study using optical analyses. *Materials Today Chemistry*, 16, 100231. <https://doi.org/10.1016/j.mtchem.2019.100231>

- [16] Aboraia, A. M., Darwish, A. A. A., Polyakov, V. A., Erofeeva, E. A., Butova, V. V., Zahran, H. Y., El-Rehim, A. F. A., Algarni, H., Yahia, I. S., & Soldatov, A. V. (2020). Structural characterization and optical properties of zeolitic imidazolate frameworks (ZIF-8) for solid-state electronics applications. *Optical Materials*, 100, 109648. <https://doi.org/10.1016/j.optmat.2019.109648>
- [17] Guo, Y., Su, J., Wang, L., Lin, Z., Hao, Y., & Chang, J. (2021). Improved Doping and Optoelectronic Properties of Zn-Doped CsPbBr₃ Perovskite through Mn Codoping Approach. *The Journal of Physical Chemistry Letters*, 12(13), 3393–3400. <https://doi.org/10.1021/acs.jpcllett.1c00611>
- [18] Chen, S., Li, M., Zhu, Y., Cai, X., Xiao, F., Tianjun, Ji, Y., Shen, G., Ke, A., Lu, Y., Liang, W., Hsu, H., Chen, C., Tang, J., & Song, H. (2022). A Codoping Strategy for Efficient Planar Heterojunction Sb₂S₃ Solar Cells. *Advanced Energy Materials*, 12(47). <https://doi.org/10.1002/aenm.202202897>
- [19] Mohamed, R. M., & Shawky, A. (2022). Visible-light-driven hydrogen production over ZIF-8 derived Co₃O₄/ZnO S-scheme based p-n heterojunctions. *Optical Materials*, 124, 112012. <https://doi.org/10.1016/j.optmat.2022.112012>
- [20] Chen, L., Wang, H., Li, C., & Xu, Q. (2020). Bimetallic metal–organic frameworks and their derivatives, *Chemical Science*, (1121), 5369–5403. <https://doi.org/10.1039/d0sc01432j>
- [21] Vatani, P., Aliannezhadi, M. & Shariatmadar Tehrani, F. (2024). Improvement of optical and structural properties of ZIF-8 by producing multifunctional Zn/Co bimetallic ZIFs for wastewater treatment from copper ions and dye. *Sci Rep* 14, 15434 . <https://doi.org/10.1038/s41598-024-66276-7>
- [22] Dolgoplova, E. A., Brandt, A. J., Ejegbavwo, O. A., Duke, A. S., Maddumapatabandi, T. D., Galhenage, R. P., Larson, B. W., Reid, O. G., Ammal, S. C., Heyden, A., Chandrashekar, M. V. S., Stavila, V., Chen, D. A., & Shustova, N. B. (2017). Electronic properties of bimetallic metal–organic frameworks (MOFs): Tailoring the density of electronic states through MOF modularity. *Journal of the American Chemical Society*, 139(14), 5201–5209. <https://doi.org/10.1021/jacs.7b01125>
- [23] Shah, S. S. A., Nazir, M. A., Mahmood, A., Sohail, M., Rehman, A. ur, Tufail, M. K., Najam, T., Javed, M. S., Eldin, S. M., Rahman, M. R., & Rahman, M. M. (2023). Synthesis of electrical conductive metal-organic frameworks for electrochemical applications. *The Chemical Record*, 24(1). <https://doi.org/10.1002/tcr.202300141>
- [24] Li, X., Wang, X., Zhou, J., Han, L., Sun, C., Wang, Q., & Su, Z. (2018). Ternary hybrids as efficient bifunctional electrocatalysts derived from bimetallic metal–organic–frameworks for overall water splitting. *Journal of Materials Chemistry A*, 6(14), 5789–5796
- [25] Nguyen, T. N., Nguyen, H. P., Kim, T., & Lee, S. W. (2018). Bimetallic Co/Zn-ZIF as an efficient photocatalyst for degradation of indigo carmine. *Korean Journal of Materials Research*, 28(1), 68–74. <https://doi.org/10.3740/mrsk.2018.28.1.68>
- [26] Xu, D., Yu, X., Jiang, X., Zhang, J., Ni, Z., & Wang, M. (2023). Synthesis of Co_xZn_{1-x} zeolitic imidazolate frameworks (ZIFs) as efficient photocatalyst with high stability, *Catalysis Communications*, 185, 106810. <https://doi.org/10.1016/j.catcom.2023.106810>
- [27] Butova, V. V., Bulanova, E. A., Polyakov, V. A., Guda, A. A., Aboraia, A. M., Viktor, S. V., Zahran, H. Y., Yahia, I. S., & Soldatov, A. V. (2019). The effect of cobalt content in Zn/Co-ZIF-8 on iodine capping properties. *Inorganica Chimica Acta*. <https://doi.org/10.1016/j.ica.2019.04.011>
- [28] Luo, X., Liang, J., Han, W., Wang, J., & Zhou, Z. (2023). Fe-and-N co-doped Fe-ZIF-8-NH₂(1/10) prepared by molecular-scale cages effect for highly efficient photocatalytic degradation of organic dyes. *Journal of Molecular Structure*, 1291, 135910. <https://doi.org/10.1016/j.molstruc.2023.135910>
- [29] Wang, H., You, H., Wu, G., Huang, L., Yan, J., Liu, X., Ma, Y., Wu, M., Zeng, Y., Yu, J., & Zhang, H. (2023). Co/Fe co-doped ZIF-8 derived hierarchically porous composites as high-performance electrode materials for Cu²⁺ ions capacitive deionization *Chemical Engineering Journal*, 460, 141621. <https://doi.org/10.1016/j.cej.2023.141621>
- [30] Mehrehjedy, A., Kumar, P., Ahmad, Z., Jankoski, P., Kshirsagar, A.S., Azoulay, J.D., He, X., Gangishetty, M.K., Clemons, T.D., Gu, X., Miao, W., & Guo, S. (2024) Fast and Facile Synthesis of Cobalt-Doped ZIF-8 and Fe₃O₄/MCC/Cobalt-Doped ZIF-8 for the Photodegradation of Organic Dyes under Visible Light. *ACS Omega*, 9(50):49239-49248. doi: 10.1021/acsomega.4c06142
- [31] Butova, V. V., Budnyk, A. P., Буланова, Е. А., Lamberti, C., & Солдатов, А. В. (2017). Hydrothermal synthesis of high surface area ZIF-8 with minimal use of TEA. *Solid State Sciences*, 69, 13–21. <https://doi.org/10.1016/j.solidstatesciences.2017.05.002>
- [32] Zheng, H., Wu, D., Wang, Y., Liu, X., Gao, P., Liu, W., Wen, J., & Rebrov, E. V. (2020). One-step synthesis of ZIF-8/ZnO composites based on coordination defect strategy and its derivatives for photocatalysis. *Journal of Alloys and Compounds*, 838, 155219. <https://doi.org/10.1016/j.jallcom.2020.155219>
- [33] Zhang, P., Zhang, X., Sun, H., Dai, X., Su, H., Qin, Y., Gao, D., Jin, A., Wang, H., Wang, X., & Sun, S. (2018). Microwave-Assisted, Ni-Induced Fabrication of Hollow ZIF-8 Nanoframes for the Knoevenagel Reaction. *Crystal Growth & Design*, 18(7), 3841–3850. <https://doi.org/10.1021/acs.cgd.8b00045>
- [34] Loloie, M., Kaliaguine, S., & Rodrigue, D. (2022). CO₂-selective mixed matrix membranes of bimetallic Zn/Co-ZIF vs. ZIF-8 and ZIF-67. *Separation and Purification Technology*, 296, 121391. <https://doi.org/10.1016/j.seppur.2022.121391>
- [35] Zhou, K., Mousavi, B., Luo, Z., Phatanasri, S., Chaemchuen, S., & Verpoort, F. (2017). Characterization and properties of Zn/Co zeolitic imidazolate frameworks vs. ZIF-8 and ZIF-67. *Journal of Materials Chemistry A*, 5(3), 952–957. <https://doi.org/10.1039/c6ta07860e>
- [36] Varsha, M., & Nageswaran, G. (2020). Review—Direct electrochemical synthesis of metal-organic frameworks. *Journal of the Electrochemical Society*, 167(15), 155527. <https://doi.org/10.1149/1945-7111/abc6c6>
- [37] Rajesh, R. U., Mathew, T., Kumar, H., Singhal, A., & Thomas, L. (2024). Metal-organic frameworks: Recent advances in synthesis strategies and applications. *Inorganic Chemistry Communications*, 162, 112223. <https://doi.org/10.1016/j.inoche.2024.112223>
- [38] Dejun, X., Zhang, Y., Jiang, X. S., Zhang, J., Ni, Z., & Wang, M. (2023). Synthesis of Co Zn_{1-x} zeolitic imidazolate frameworks (ZIFs) as efficient photocatalyst with high stability. *Catalysis Communications*, 185, 106810. <https://doi.org/10.1016/j.catcom.2023.106810>
- [39] Abdi, J. (2020). Synthesis of Ag-doped ZIF-8 photocatalyst with excellent performance for dye degradation and antibacterial activity. *Colloids and Surfaces A Physicochemical and engineering Aspects*, 604, 125330. <https://doi.org/10.1016/j.colsurfa.2020.125330>

- [40] Yan, P., Li, X., Ma, D., Li, L., Lan, Y., Li, Z., Lu, X., Yang, M & Liang, L. (2022). A cobalt-based MOF with the synergistic effect of size sieving and multi-functional sites for selective gas adsorption, *Journal of Solid State Chemistry*, 316, 123566. <https://doi.org/10.1016/j.jssc.2022.123566>
- [41] Sebastiana, A., Vandana, P., Josepha, A., Xavier, M.M. & Mathewa, S. (2017). Metal-organic frameworks: Optoelectronic properties and its applications, *Sci. Adv. Today*, **3**, 25263.
- [42] Jing, Y., Qiang, L., Xia, C., Wang, D., Yang, Y., He, J., Yang, Y., Zhang, Y., & Yan, M. (2020). Synthesis of Ag and AgCl co-doped ZIF-8 hybrid photocatalysts with enhanced photocatalytic activity through a synergistic effect. *RSC Advances*, 10(2), 698–704. <https://doi.org/10.1039/c9ra10100d>
- [43] Tuncel, D., & Ökte, A. N. (2021). Improved adsorption capacity and photoactivity of ZnO-ZIF-8 nanocomposites. *Catalysis Today*, 361, 191–197. <https://doi.org/10.1016/j.cattod.2020.04.014>
- [44] Zafar, Z., Yi, S., Li, J., Li, C., Zhu, Y., Zada, A., Yao, W., Liu, Z., & Yue, X. (2022). Recent development in defects engineered photocatalysts: An overview of the experimental and theoretical strategies. *Energy and Environmental Materials*, 5, 68–114. <https://doi.org/10.1002/eem2.1217>
- [45] Gawali, S., Gandhi, A. C., Gaikwad, S. S., Pant, J., Chan, T.-S., Cheng, C.-L., Ma, Y.-R., & Wu, S. Y. (2018). Role of cobalt cations in short range antiferromagnetic Co₃O₄ nanoparticles: A thermal treatment approach to affecting phonon and magnetic properties *Scientific reports*, 8(1), 249. <https://doi.org/10.1038/s41598-017-18563-9>
- [46] Lim, G. J. H., Liu, X., Guan, C., & Wang, J. (2018). Co/Zn bimetallic oxides derived from metal organic frameworks for high performance electrochemical energy storage. *Electrochimica Acta*, 291, 177–187. <https://doi.org/10.1016/j.electacta.2018.08.105>
- [47] Baghban, A., Habibzadeh, S., & Ashtiani, F. Z. (2020). Bandgaps of noble and transition metal/ZIF-8 electro/catalysts: a computational study. *RSC Advances*, 10(39), 22929–22938. <https://doi.org/10.1039/d0ra02943b>
- [48] Tian, T., Scullion, D., Hughes, D., Li, L. H., Shih, C., Coleman, J. N., Chhowalla, M., & Santos, E. J. G. (2019). Electronic polarizability as the fundamental variable in the dielectric properties of two-dimensional materials. *Nano Letters*, 20(2), 841–851. <https://doi.org/10.1021/acs.nanolett.9b02982>
- [49] Lu, Y., Li, M., Yu F, Xu, Y., Zhou, Y., Ji, X., & Wang, J. (2024). Tuning the optical properties of transparent ZIF-8 thin films by adjusting the crystal morphology. *Optical Materials*, 154, 115714–115714. <https://doi.org/10.1016/j.optmat.2024.115714>
- [50] Saliba, D., Ammar, M., Rammal, M., Al-Ghoul, M., & Hmadeh, M. (2018). Crystal growth of ZIF-8, ZIF-67, and their mixed metal derivatives. *Journal of the American Chemical Society*, 140(5), 1812–1823. <https://doi.org/10.1021/jacs.7b11589>
- [51] Onochie, U.P., Ikpeseni, S.C., Owamah, H.I., Iweoko, A.E., Ukala, D.C., Nwaigwe, U.S. Augustine, C. (2021): Analysis of optical band gap and Urbach tail of zinc sulphide coated with aqueous and organic dye extracts prepared by chemical bath deposition technique. *Optical Materials*, 114(2021) 110970. <https://doi.org/10.1016/j.optmat.2021.110970>
- [52] Saive, R. (2021). Light trapping in thin silicon solar cells: A review on fundamentals and technologies. *Progress in photovoltaics research and applications*, 29(10), 1125–1137. <https://doi.org/10.1002/ppp.3440>
- [53] Amalathas, A. P., & Alkaisi, M. M. (2019). Nanostructures for light trapping in thin film solar cells. *Micromachines*, 10(9), 619–619. <https://doi.org/10.3390/mi10090619>
- [54] Keppler, N., Hindricks, K. D. J., & Behrens, P. (2022). Large refractive index changes in ZIF-8 thin films of optical quality. *RSC Advances*, 12(10), 5807–5815. <https://doi.org/10.1039/d1ra08531j>
- [55] Onochie, U.P., Ikpeseni, S.C., Iweoko, A.E., Owamah, H.I., Aluma, C.C., Augustine, C. (2021): Optical properties of Zinc sulphide thin films coated with aqueous organic dye extract for solar and optoelectronic device applications. *Journal of Elec. Materi* (2021). <https://doi.org/10.1007/s11664-021-08792-0>.
- [56] Aulia, W., Ahnaf, A., Irianto, M. Y., Ediati, R., Iqbal, R. M., Rachman, R. A., & Martia, U. T. I. (2020). Synthesis and characterization of zeolitic imidazolate framework-8 (ZIF-8)/Al₂O₃ composite. *Iptek/Majalah IPTEK Institut Teknologi Sepuluh Nopember 1945 Surabaya*, **31**(1), 18. <https://doi.org/10.12962/j20882033.v31i1.5511>
- [57] Awadallah-F, A., Hillman, F., Al-Muhtaseb, S. A., & Jeong, H. (2019). Influence of doped metal center on morphology and pore structure of ZIF-8. *MRS Communications*, 9(1), 288–291. <https://doi.org/10.1557/mrc.2018.221>
- [58] Eslava, S., Zhang, L., Esconjauregui, S., Yang, J., Vanstreels, K., Baklanov, M. R., & Saiz, E. (2012). Metal-organic framework ZIF-8 Films As low-κ dielectrics in microelectronics. *Chemistry of Materials*, 25(1), 27–33. <https://doi.org/10.1021/cm302610z>
- [59] Liu, S., Liu, C., Bai, Z., Lin, G., & Liu, X. (2023). Metal-organic frameworks mediated interface engineering of polymer nanocomposites for enhanced dielectric constant and low dielectric loss. *Surfaces and Interfaces*, 36, 102586. <https://doi.org/10.1016/j.surfin.2022.102586>
- [60] Fu, Z., Zhang, X., Zhang, H., Li, Y., Zhou, H., & Zhang, Y. (2020). On the understandings of dielectric constant and its impacts on the photovoltaic efficiency in organic solar cells. *Chinese Journal of Chemistry*, 39(2), 381–390. <https://doi.org/10.1002/cjoc.202000289>